

Catastrophic extinction, noise-stabilized turbulence and unpredictability of competition in a modified Volterra–Lotka model

A. B. Goryachev, A. A. Polezhaev, and D. S. Chernavskii

I. E. Tamm Theoretical Department, P. N. Lebedev Physical Institute, Leninskiy prospect 53, 117924 Moscow, Russia

(Received 5 April 1995; accepted for publication 14 September 1995)

Spatial coexistence and competition among species is investigated through a modified Volterra–Lotka model which takes into account sexual breeding. This allows the population specific growth rate to depend on the population density. As a result of this modification the degeneracy inherent in the classical model is eliminated and qualitatively novel regimes are observed, as demonstrated by parametric analysis of the model. In the case where the corresponding parameters of competing species do not differ significantly the model can be reduced to a single Ginzburg–Landau type equation. The spatially distributed model is analyzed both in the absence and in the presence of noise mimicking inherent fluctuations in birth and death rates. It is shown that noise can qualitatively change the behavior of the system. Not only does it induce the formation of spatial patterns, but also switches on endless turbulent-like rearrangement of the system. When initially unpopulated habitat is occupied by competing species even a very low-intensity noise makes the final state of the system totally unpredictable and sensitive to any fluctuations. © 1996 American Institute of Physics. [S1054-1500(96)00101-7]

I. INTRODUCTION

The problem of biological pattern formation and in particular of spatial patterns formed by living populations has been a matter of scientific interest for a long time. Various mechanisms have been proposed to account for the emergence and stability of mosaic patterns typical of natural ecosystems when they cannot be simply attributed to the heterogeneity of the environment. As one of the explanations of these phenomena dissipative structures were suggested for the well-studied class of predator-prey models.^{1,2} Although predation has been shown to play an important role in the spatial organization of ecosystems, it is not the sole source of self-emerging inhomogeneity. Another fundamental biological interaction, namely competition, acting on all levels of biological organization from individuals to ecosystems, seems to be equally or (due to its global ubiquity) even more responsible for the formation of spatial patterns.

The standard Volterra–Lotka type model describing competition between two species takes the form first introduced by Gause³:

$$\begin{aligned}\dot{N}_1 &= N_1(k_1 - a_{11}N_1 - a_{12}N_2), \\ \dot{N}_2 &= N_2(k_2 - a_{21}N_1 - a_{22}N_2),\end{aligned}\quad (1)$$

where N_1 , N_2 are the population densities, k_i are the Malthusian coefficients, and a_{ij} , a_{ij} ($i, j=1,2$) are those of intra- and interspecific competition respectively. To describe random migration of individuals in continuous habitats, it is conventional⁴ to introduce diffusion-like terms into Eqs. (1). However, any nonuniform spatial solution of the model (1) is unstable. This can be understood qualitatively from the inherent principle of competition—“winner takes all.”

Significant efforts have been made to find additional mechanisms, not allowed for by the classical model, which

can maintain the observed stability of spatial patterns. It was suggested^{5–7} that species migrate due to self- and cross-diffusion with the motility being a function of N_i and increasing in regions of high population density. The formation of stable patterns in this case was reported in Ref. 7. Another approach was worked out by Britton,^{8,9} who assumed that individuals tend to aggregate and that competition terms involve nonlocal interactions. Therefore, effective short-range activation and long-range inhibition essential for dissipative structure formation were introduced providing pattern stability. Both approaches imply that individuals can move intentionally through the habitat, and consequently, diffusion fails to represent their complex motion. This means that the latter models can be applied only to animal species. However, it is plants that give the most spectacular examples of spatial patterns.

In the present paper a modification of the classical model (1) is proposed. Instead of assuming nonlinear diffusion and nonlocal interaction effects we concentrate on specification of the local population dynamics. Section II is devoted to the formulation and parametric analysis of the modified model. The replacement of some simplistic assumptions concerning species growth by those taking into account sexual breeding makes the model structurally stable and enriches its dynamic behavior. By reducing the model to a single Ginzburg–Landau type equation for the effective order parameter, the problem is shown in Sec. III to be one of the many multistable systems abundant in physical sciences. Various consequences from the application of noise mimicking inherent fluctuations in birth and death rates are presented in Sec. IV. The most prominent one among them is that noise is responsible for initiation and support of spatio-temporal patterns arising in the model. The influence of noise on various dynamical systems has been studied extensively (see, e.g. Refs.

10 and 11 and references therein). However, only few sufficiently simple problems (mostly with additive noise) can be solved exactly. According to Ref. 10, pattern formation in the stochastic models remains one of the most complex and unexplored domains where very often the only fruitful way to gain insight is through numerical simulation. The case of multiplicative noise in a spatially distributed dynamical system with multistable potential, being considered in the present paper, evidently belongs to this problem domain and to the best of our knowledge has not been yet studied in the literature in the context of population dynamics models to be discussed. In Sec. V we touch upon the problem of natural selection. It is conventionally believed that its main principle can be briefly formulated as "survival of the fittest." However, determining the strongest species is not intuitively obvious because of the numerous parameters that come into play. Indeed, the role of chance is shown to be significant in this situation. In Sec. VI the properties of the modified model are compared to those of the classical one. It is inferred that noise plays an organizing rather than destabilizing role.

II. COMPETITION OF SEXUALLY BREEDING SPECIES

One of the basic assumptions of the classical Volterra–Lotka type model (1) is that of the independence of the population growth rate on the population density. For sexually breeding species such an assumption is valid only at sufficiently high population densities. Otherwise the probability of mating (i.e. of finding a breeding partner) may drop significantly, leading to an effective decrease in an individual fertility. Let us consider a population of some species which has sexual breeding along with a vegetative one, and let $2n$ be the number of offsprings produced by any female individual in a unit time. Then if both sexes are equally presented in the population, the number δN of individuals born in time δt will be

$$\delta N = (n \cdot p(N) + k)N \delta t.$$

Assuming the partner search process to be a Poisson one, the probability of mating becomes $p(N) = 1 - \exp(-\lambda N)$. Then the Malthusian function of the population reads as $G(N) = N \cdot g(N) = N \cdot (k + n(1 - \exp(-\lambda N)))$. For large N this function tends to its classical scaling $\sim N$, but for low N the sexual breeding contribution is proportional to N^2 , thereby explicitly showing the cooperative nature of sexual breeding. The mating probability function of this type is often approximated by the rational function $N/(\lambda^{-1} + N)$. For simplicity we also use this approach. This form of $p(N)$ supposes the mating behavior of individuals to be very simple and to a large extent passive. Moreover, because genetic material, e.g. pollen, can be randomly dispersed by wind or water mating behavior as such becomes nonexistent. Thus, the above Malthusian function probably fits well to the majority of plants and some simple animals like hydroid polyps.

Another mating strategy common for animals with a well developed tendency to aggregation, is described by the Alle-type population dynamics.¹² It is more convenient to

use the individual fertility function $g(N) = G(N)/N$ than the Malthusian function $G(N)$ itself. For the Alle-type population $g(N)$ has the characteristic sigmoid shape. Initially increasing slowly, $g(N)$ grows significantly in the vicinity of some critical value N_c until it saturates, similar to the case discussed earlier. The critical value N_c corresponds to the population density at which individuals actively aggregate in swamps, schools, flocks, etc.

The two types of Malthusian functions mentioned above cover the majority of all cases occurring in nature. Taking into account the dependence of the individual fertility function on the population density N we obtain instead of (1)

$$\begin{aligned} \dot{N}_1 &= N_1(g_1(N_1) - aN_1 - N_2), \\ \dot{N}_2 &= N_2(g_2(N_2) - N_1 - bN_2). \end{aligned} \quad (2)$$

Though rigorous analysis of Eqs. (2) for arbitrary g_1 and g_2 is difficult, the character of stationary points of the set (2) can be easily derived from a simple geometrical investigation of nullclines intersecting in these points. Isoclines of the model (2) split into four branches, two of them being the axes $N_1 = 0$ and $N_2 = 0$, and may intersect in many different ways. Depending on the type of $g(N)$ and the parameters, the number of singular points varies from 2 to 13. Let us first consider the stationary points $N_1 = \tilde{n}_1$, $N_2 = \tilde{n}_2$, situated in the interior of the positive quadrant $N_1, N_2 > 0$. Linearizing Eqs. (2) in the neighborhood of the chosen point we obtain for the eigenvalues:

$$\begin{aligned} \lambda_{1,2} &= 0.5(-(\tilde{n}_1 k_1 + \tilde{n}_2/k_2) \\ &\quad \pm \sqrt{(\tilde{n}_1 k_1 + \tilde{n}_2/k_2)^2 + 4\tilde{n}_1 \tilde{n}_2}), \end{aligned} \quad (3)$$

where $k_1 = g'_1(\tilde{n}_1) - a$ and $k_2 = g'_2(\tilde{n}_2) - b$ are inclinations of the corresponding nullclines to the axis $N_2 = 0$.

From Eq. (3) it is evident that the eigenvalues are always real. This result can be easily extended on any competition model with arbitrary right parts $F_1(N_1, N_2), F_2(N_1, N_2)$ providing that $\partial F_1/\partial N_2, \partial F_2/\partial N_1 < 0$. Multiplying the eigenvalues (3) we obtain the clear classification rule for the internal stationary points

$$\lambda_1 \lambda_2 = \tilde{n}_1 \tilde{n}_2 (k_1/k_2 - 1).$$

From this we see that the nature of a singular point is completely determined by the inclinations of nullclines in the point. Namely it is

- a stable node, if $k_1 < k_2 < 0$,
- an unstable node, if $k_1 > k_2 > 0$,
- a saddle in the other cases.

To consider singular points lying on the border we assume $\tilde{n}_2 = 0$ (the case $\tilde{n}_1 = 0$ can be treated in the same way). Eigenvalues for the corresponding linear problem in this case can be calculated explicitly:

$$\begin{aligned} \lambda_1 &= \tilde{n}_1 k_1, \\ \lambda_2 &= g_2(0) - \tilde{n}_1. \end{aligned}$$

This immediately results in the following criterion. If $\tilde{n}_1 > 0$ and $\tilde{n}_2 = 0$, a singular point on the border of the positive quadrant is

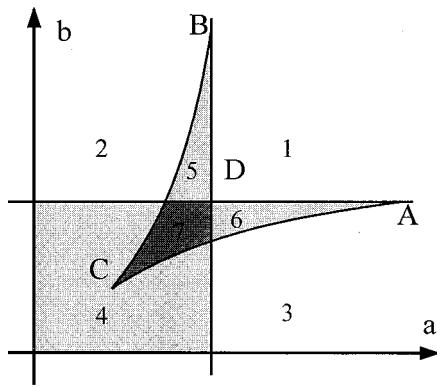


FIG. 1. Partitioning of the parametric space for the model (4). Background intensity reflects the number of stationary stable states: white —1, light grey —2, dark grey —3.

- a stable node, if $k_1 < 0, \tilde{n}_1 > g_2(0)$,
- an unstable node, if $k_1 > 0, \tilde{n}_1 < g_2(0)$,
- a saddle in the other cases.

The classification rules obtained solve in principle the problem of model (2) qualitative analysis, since not only for both classes of $g(N)$ mentioned above but also for any competition model with arbitrary right hand parts $F_1(N_1, N_2), F_2(N_1, N_2)$ and $\partial F_1 / \partial N_2, \partial F_2 / \partial N_1 < 0$ it can be easily shown that stationary points are the only permitted singularities (see the Appendix).

From this point onward, we will consider fertility functions of the first type only. Substituting functions $g_i(N_i)$ in the set (2) by their rational approximation in the form $k_{i,1} + k_{i,2}N_i / (N_i + \gamma_i)$, after a little manipulation we obtain for the dimensionless population densities n_1 and n_2 :

$$\begin{aligned} \dot{n}_1 &= n_1 \left(1 + \rho - \frac{\alpha_1 \beta_1}{n_1 + \alpha_1} - a n_1 - n_2 \right), \\ \dot{n}_2 &= n_2 \left(1 - \rho - \frac{\alpha_2 \beta_2}{n_2 + \alpha_2} - n_1 - b n_2 \right). \end{aligned} \tag{4}$$

The model (4) incorporates the classical one in the limiting case when $\alpha_i, \beta_i \rightarrow 0$. Close investigation of (4) shows that for all sensible combinations of ρ, α_i, β_i , continuous varying of the competition parameters a and b results in topologically the same configurations of nullcline intersections and thus for qualitatively equivalent phase portraits. This enables one to investigate all the generic cases assuming parameters a, b are variable and the others fixed at some arbitrary values. Then the partitioning of the (a, b) parametric plane into domains where the model (4) has qualitatively the same phase portraits is shown in Fig. 1. Region 1 corresponds to the only stable stationary state of the model situated in the interior of the positive quadrant indicating stable coexistence of species. This contrasts with domains 2 and 3 where only one species survives for any initial conditions. Following a definite analogy to physics, it is convenient to refer to the stationary states of stable coexistence as “mixed” ones, assuming that “pure” states correspond to the presence of only one of the species. In the domain 4 both pure states are

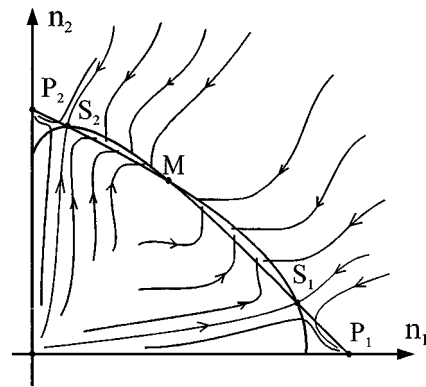


FIG. 2. Phase portrait typical of the tri-stable parameter domain. P_1, P_2 —pure, M —mixed, S_1, S_2 —saddle states.

stable, the mixed one being a saddle point. All the domains mentioned so far are also typical of the classical model with linear nullclines while others are specific only for the model (4). Two stable stationary states exist in the domains 5 and 6, but unlike region 4, one of them is mixed. Consequently, coexistence becomes sensitive to the initial conditions for the parameters lying in these domains. Finally, in domain 7 both pure states and the mixed one are simultaneously stable. The phase portrait for this case is presented in Fig. 2.

Special attention should be paid to the curve ACB where species coexistence abruptly breaks down. On this curve the stable node corresponding to the coexistence of species annihilates with the saddle leading to catastrophic extinction of one of the species. The closer such a catastrophe occurs to the point C , the larger the jump undergone by the ecosystem. The location of the catastrophic curve ACB on the (a, b) plane can be derived from the condition that nullclines are tangent in the point of their intersection:

$$\begin{aligned} 1 + \rho - \frac{\alpha_1 \beta_1}{n_1 + \alpha_1} - a n_1 - n_2 &= 0, \\ 1 - \rho - \frac{\alpha_2 \beta_2}{n_2 + \alpha_2} - n_1 - b n_2 &= 0, \end{aligned} \tag{5}$$

$$\left(\frac{\alpha_1 \beta_1}{(n_1 + \alpha_1)^2} - a \right) \left(\frac{\alpha_2 \beta_2}{(n_2 + \alpha_2)^2} - b \right) = 1.$$

It is apparently difficult to solve this system rigorously. Let us instead examine the character of the solution using perturbation technique in the vicinity of the point C only. For simplicity we consider a symmetrical case $\alpha_1 = \alpha_2, \beta_1 = \beta_2, \rho = 0$. Decomposing a, b, n_1 and n_2 into power series near the point C after a little manipulation we obtain from Eqs. (5) :

$$\begin{aligned} a &= a_c + \varepsilon^2 a_2 + \varepsilon^3 a_3, \\ b &= b_c + \varepsilon^2 b_2 + \varepsilon^3 b_3, \\ a_c &= b_c, \quad a_2 = b_2, \quad a_3 \neq b_3. \end{aligned}$$

Placing the origin in the (a, b) plane into the point C and rotating the axes so that $\tilde{a} = a + b - (a_c + b_c), \tilde{b} = a - b$ after

exclusion of ε we obtain $\tilde{b}^2 \sim \tilde{a}^3$. Such a behavior is specific for a bifurcation set of a cusp catastrophe. If we were able to construct an appropriate scalar value reflecting species composition (see the next section for this procedure in the vicinity of C) and then plot it in the 3-D space against the parameters a and b , we would get a catastrophe manifold of the model (4). The projection of its bifurcation set on the (a, b) plane partitions it into domains as is shown in Fig. 1. Three cusp catastrophes connected by the curve of fold ones (thick solid line in Fig. 1) project into the points A , B and C . In each of them three stationary points of the model (4) merge. The neighborhood of C is of particular interest. Being locally stable and nontrivial (in the sense that densities of both species are far from zero) the state of coexistence becomes sensitive to large amplitude perturbations which can lead to the abrupt extinction of one of the competing species.

III. SPATIALLY DISTRIBUTED HABITATS

Let us now consider species competing in a continuous, large enough but finite, one dimensional habitat, where individuals are able to migrate (or disperse seeds) randomly. In this case the model takes the form of a set of reaction-diffusion equations

$$\begin{aligned} \dot{n}_1 &= n_1 \left(1 + \rho - \frac{\alpha_1 \beta_1}{n_1 + \alpha_1} - a n_1 - n_2 \right) + D_1 \Delta n_1, \\ \dot{n}_2 &= n_2 \left(1 - \rho - \frac{\alpha_2 \beta_2}{n_2 + \alpha_2} - n_1 - b n_2 \right) + D_2 \Delta n_2, \end{aligned} \quad (6)$$

where the motility coefficients D_1, D_2 are assumed to be constant, and the boundary conditions are of the Neumann type. If natural competition is implied one should expect only small differences between the corresponding parameters of rivals, i.e. $a \approx b, \rho \approx 0, D_1 \approx D_2$. Otherwise one of the species will occupy the whole habitat causing the other to be extinct. Thus, to avoid unnecessary complication of the model (6), D_1 and D_2 are considered equal: $D_1 = D_2 = D$. The parameter D can then be excluded from Eqs. (6) by rescaling of the spatial coordinate.

Although the set (6) is complex for analysis, it can be reduced in some neighborhood of the point C in the parametric space to a single equation for the effective system order parameter. The idea of this transform may be easily seen from Fig. 2. If a and b lie close to the cusp point C inside the tri-stable domain 7, all the nontrivial stationary states are situated in the line which coincides with α -separatrices connecting the saddle points. Since motion along this curve composed of separatrices (not shown in Fig. 2) is much slower than toward it, one may expect the problem to become effectively one dimensional. To avoid complicated computations, we further simplify Eqs. (6) setting $\alpha_1 = \alpha_2 = \alpha, \beta_1 = \beta_2 = \beta, \rho = 0, a = b$. Let $n_1 = n_2 = \bar{n}$ be the coordinates of the stable mixed state. Then in the variables $u_1 = n_1 - \bar{n}, u_2 = n_2 - \bar{n}$, measuring deviations of n_1 and n_2 from the stationary state, Eqs. (6) take the form

$$\begin{aligned} \dot{u}_1 &= Q u_1 - \bar{n} u_2 - a u_1^2 - u_1 u_2 + \frac{\alpha^2 \beta u_1^2}{(\bar{n} + \alpha)^2 (u_1 + \bar{n} + \alpha)} \\ &\quad + \Delta u_1, \\ \dot{u}_2 &= Q u_2 - \bar{n} u_1 - a u_2^2 - u_1 u_2 + \frac{\alpha^2 \beta u_2^2}{(\bar{n} + \alpha)^2 (u_2 + \bar{n} + \alpha)} \\ &\quad + \Delta u_2, \end{aligned} \quad (7)$$

where

$$Q = 1 - (1 + 2a)\bar{n} - \frac{\alpha^2 \beta}{(\bar{n} + \alpha)^2}.$$

In the vicinity of the cusp point we may take $a = a_c + \varepsilon, \bar{n} = \bar{n}_c + \varepsilon \bar{n}_1 + \dots$. In addition we assume the nonlinearity of nullclines to be local, i.e. $\alpha \ll 1$. Thus, all the coefficients in the ε -series may be further expanded into the power series of α . Omitting terms nonlinear in ε and α we obtain from Eqs. (5)

$$\begin{aligned} a &= 1 + 4\alpha\beta + \varepsilon + O(\alpha^2, \varepsilon^2, \alpha\varepsilon), \\ \bar{n} &= 1 - 2\alpha\beta - \varepsilon/2 + O(\alpha^2, \varepsilon^2, \alpha\varepsilon). \end{aligned}$$

Substituting these expressions into Eqs. (7) and solving the characteristic equation we find the eigenvalues to be: $\lambda_1 = -\varepsilon/2 + O(\alpha^2, \varepsilon^2, \alpha\varepsilon), \lambda_2 = -1 + O(\alpha^2, \varepsilon^2, \alpha\varepsilon)$. Directing axes along the corresponding eigenvectors one gets a change of variables $q = u_1 - u_2, v = u_1 + u_2$. With these new variables the set (7) takes the form:

$$\begin{aligned} \dot{v} &= -v - v^2 - (2\alpha\beta + \varepsilon/2)q^2 + 4\alpha^2\beta \frac{v^3 + v^2 - q^2v + q^2}{v^2 + 2v + 1 - q^2} \\ &\quad + \Delta v, \\ \dot{q} &= -\frac{\varepsilon}{2}q - qv + 4\alpha^2\beta \frac{v^2q - q^3 - qv/2}{v^2 + 2v + 1 - q^2} + \Delta q, \end{aligned} \quad (8)$$

where unessential terms are omitted. The fast stable variable v can be excluded from (8) by means of conventional procedure.¹³ Solution of $\dot{v} = 0$ gives

$$v = -(\varepsilon/2 + 2\alpha\beta)q^2.$$

In view of this, after some manipulation we obtain the equation for the order parameter field $q(x, t)$

$$\dot{q} = \frac{q(q^2 - 1)(\varepsilon/2 - (\varepsilon/2 + 2\alpha\beta)q^2)}{(1 + 4(1 - \beta)\alpha)^2 - q^2} + \Delta q, \quad (9)$$

which has the form of the time-dependent Ginzburg-Landau equation. Stable stationary states of the undistributed model (4) correspond to the stable phases of the spatially distributed one. In our case the roots $q_{1,2} = \pm 1$ represent stable pure phases, $q_3 = 0$ corresponds to the mixed phase, stable for $\varepsilon > 0$ and unstable otherwise. Two roots $q_{4,5} = \pm 1/2\sqrt{\varepsilon/\alpha\beta}$ represent saddle states merging at $\varepsilon = 0$.

Multistable systems of this type (mostly bistable ones) are well studied. It is known that in the general case phases cannot coexist — interphase boundaries move along the medium. Thus propagation of the kink-type fronts switching the

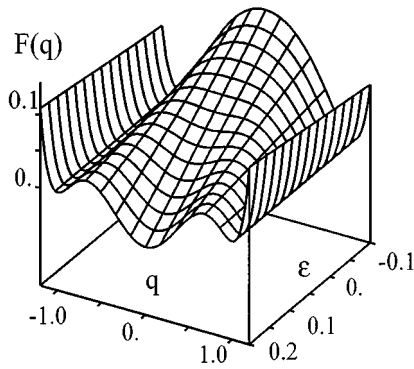


FIG. 3. The shape of the potential $F(q)$ as a function of the parameter ϵ .

medium from one state into the other is characteristic for the dynamic behavior of such a system. The convenient way to decide on the relative stability of phases is provided by the potential $F(q)$ determined by

$$f(q) = -\frac{dF(q)}{dq},$$

where $f(q)$ is the nonlinear function in Eq. (9). The shape of the potential $F(q)$ for Eq. (9) is presented in Fig. 3. The conditions for coexistence of phases i and j

$$F(q_i) = F(q_j), \quad i, j = 1, 2, 3$$

(see, e.g., Ref. 14) determine the phase balance curves in the (a, b) parametric plane. They intersect in the triple point where $F(q_1) = F(q_2) = F(q_3)$. The phase diagram for the model under consideration is schematically shown in Fig. 4. Coexistence curves terminate in the critical points A and B where, as it is shown above, the system catastrophe manifold has cusp singularities.

The only type of spatial inhomogeneities allowed are structures formed by domains of different phases, which in a 2-D medium have a characteristic parquet-like mosaic appearance. Though unstable in the frame of the deterministic model (6), these structures can be rather long-living formations¹⁵ and should not be disregarded as biologically insignificant.

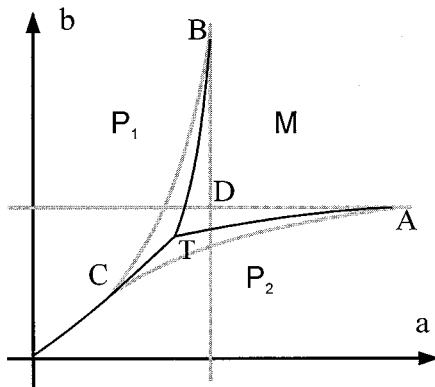


FIG. 4. Phase diagram. Bifurcation map is shown in grey for reference.

IV. COMPETITION IN THE PRESENCE OF NOISE

One of the most prominent predictions of the deterministic model is the presence of hysteresis phenomena for parameters lying inside the multistable domains. Therefore to determine the stationary state of the system, one should first define the initial conditions. The direct consequence of hysteresis is the phenomenon of metastability. Let us consider one example. Although the mixed phase is absolutely stable (for any finite perturbation) only in the region prescribed by the phase diagram (see Fig. 4), it preserves linear stability up to the ACB curve. Thus, inside the $ACBT$ domain the mixed phase remains metastable, and a nucleus of supercritical size is needed to initiate switching of the medium into one of the pure states. This picture is true, of course, only if fluctuations are disregarded completely.

One way to take into account the fluctuations in birth and death rates is to assume that the species densities n_1 and n_2 at any time and point in the medium undergo uncorrelated random pushes. For the order parameter q this gives

$$q(x, t) = \tilde{q}(x, t) + \sigma \xi(x, t), \quad (10)$$

where $\sigma^2 \ll 1$ and $\xi(x, t)$ is a random process with vanishing correlation time and length. For simplicity this is often considered to be a Poisson white noise:

$$\begin{aligned} \xi\langle(x, t)\rangle &= 0, \\ \langle\xi(x, t)\xi(x', t')\rangle &= \sigma^2 \delta(t - t') \delta(x - x'). \end{aligned}$$

Substituting (10) into Eq. (9) we obtain the Langevin equation containing the stochastic force term $L(\tilde{q})\xi$. Since $f(q)$ is a nonlinear function and therefore $L(\tilde{q}) \equiv 1$, it is a case of multiplicative internal noise. It was shown¹⁶ that in such a case the influence of noise should be manifested in two different ways. First, even very low noise shifts the deterministic bifurcation maps tending to reduce the hysteresis loops. Second, being multiplicative the noise can change the form of the system potential $F(q)$ sometimes leading to new bifurcations, which in the absence of noise would be impossible.

Further investigations of the model with the applied noise were carried out numerically. The most convenient and sensitive way to find noise-induced effects is to run down the order parameter probability density distribution (PDD) $P(q, t)$. Let a continuous medium be considered as a set of N diffusively connected boxes, and $n(q, \Delta q, t)$ be the number of them where $q \in (q, q + \Delta q)$ at the moment t , then

$$P(q, t) = \lim_{\substack{N \rightarrow \infty \\ \Delta q \rightarrow 0}} \frac{n(q, \Delta q, t)}{N \Delta q}. \quad (11)$$

It should be noted that unlike the common definition of probability density distribution, N boxes being diffusively connected do not constitute an ensemble of statistically independent systems. For the completely deterministic case ($\sigma \equiv 0$) there exist only three stationary asymptotically stable distribution functions: $P_i(q) = \delta(q - q_i)$, $i = 1, 2, 3$; with any other function $P(q, t)$ tending to one of them when $t \rightarrow \infty$. As it was stated earlier, inside the multistable domains $P(q)$ is a

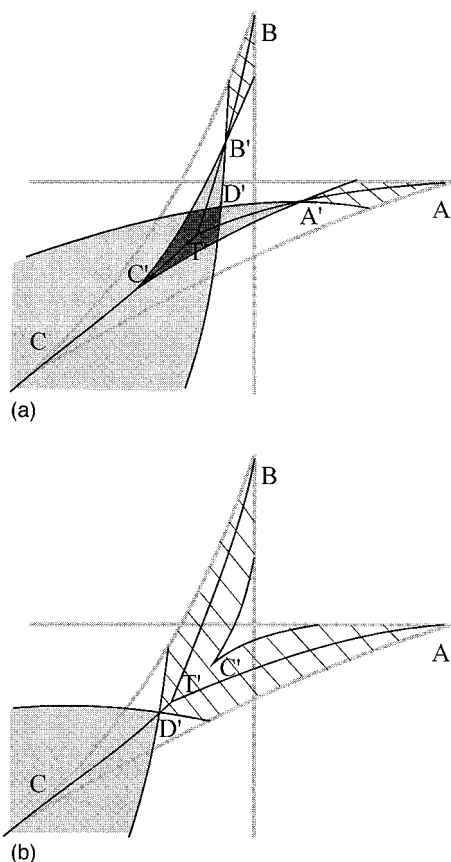


FIG. 5. Transformation of the bifurcation map in the presence of noise. (a) $\sigma^2 < \sigma_c^2$, (b) $\sigma^2 > \sigma_c^2$. Hatched area is the region of overbarrier noise. Other designations are the same as in Fig. 1.

multifunction of parameters a and b and transitions $P_i(q) \rightarrow P_j(q)$, $i, j = 1, 2, 3$, take place on the corresponding domain boundaries.

The application of noise with the intensity $\sigma^2 > 0$ allows the system to escape from shallow potential minima. Therefore the curves on the bifurcation map where the system jumps out of noise-destabilized states are no more coincident with the ones on which corresponding potential minima disappear altogether. The destabilizing effect of noise makes all the multistable regions shrink as is shown in Fig. 5a. The domain $A'C'B'D'$ geometrically similar to the $ACBD$ one also inherits all the physical properties of the latter under a completely deterministic description. With the increase of noise intensity vertices A', C', B' move along the corresponding phase balance curves in such a way that at some $\sigma^2 = \sigma_c^2$ they merge with the triple point T' and the $A'C'B'D'$ domain disappears completely.

The influence of noise is not restricted to the phase destabilization. As it can be predicted from its multiplicative nature, noise affects the very shape of the potential, shifting the positions of its minima and slightly changing their depths. Therefore the positions of phase balance curves and of the triple point are also functions of σ^2 . Figure 6 represents numerical data showing the positions of C' and the

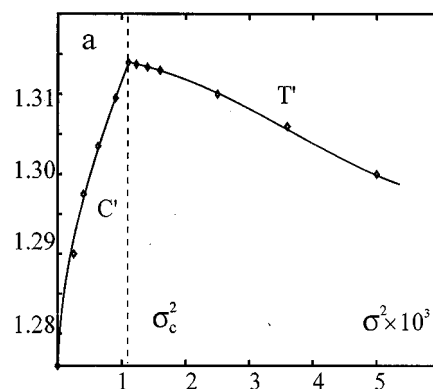


FIG. 6. Numerical simulation data for the C' and T' points positions versus noise intensity; $\alpha_1 = \alpha_2 = 0.3, \beta_1 = \beta_2 = 0.6, \rho = 0, a = b$.

triple T' points versus noise intensity σ^2 for $\alpha_1 = \alpha_2 = 0.3, \beta_1 = \beta_2 = 0.6, a = b$.

The most interesting noise-dependent phenomena, however, take place in those parametric regions where the system potential $F(q)$ has multiple minima but noise overrides all the barriers separating them (hatched area in Fig. 5). Such regions will be referred to as areas of overbarrier noise. In their interior hysteresis breaks down, and instead of a set of stationary $P(q)$ functions [which are noise-broadened and noise-shifted analogs of $P_i(q) = \delta(q - q_i)$, $i = 1, 2, 3$] we obtain a unique but multimodal order parameter probability density distribution. In this case the shape of $P(q)$ provides exhaustive information about the positions and relative depths of the $F(q)$ minima. With the increase of σ^2 these regions grow, and at $\sigma^2 = \sigma_c^2$ they conjugate in the triple point T' forming one simply connected domain, which grows further at $\sigma^2 > \sigma_c^2$ (see Fig. 5b).

In the spatio-temporal behavior of the system, the multimodality of $P(q)$ manifests itself in the broken spatial symmetry. Being diffusively connected, points of continuous medium are bound to act coherently. Therefore the medium splits into patches of different phases as is demonstrated in Fig. 7. The better the different peaks of $P(q)$ are resolved, the more noticeable the spatial inhomogeneity. On the boundaries separating the domain of overbarrier noise from

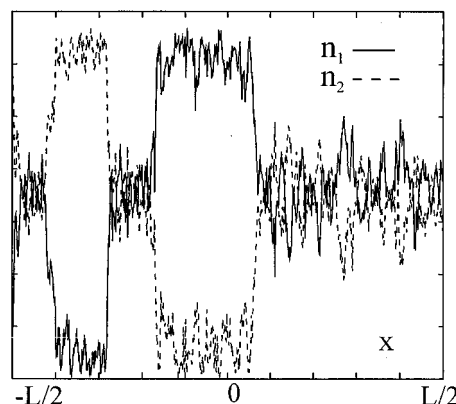


FIG. 7. An example of noise-induced domain structure.

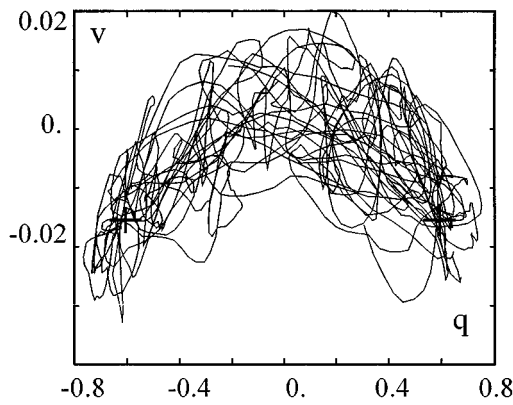


FIG. 8. Chaotical point trajectory typical of the turbulent dynamics, $\sigma=0.07$. Crosses show the positions of noise-shifted “pure” states.

those where at least one phase remains stable to noise the system can demonstrate purely noise-induced transitions from homogeneous to spatially inhomogeneous multiphase state. It should be noted that unlike the completely deterministic case, the spatial structure is not merely a transient state to spatial homogeneity. Noise initiating formation of spatial structures also stabilizes them in the sense that $P(q)$ preserves its multimodality with time. The actual species densities $n_1(x,t), n_2(x,t)$, of course, continuously change, being in endless turbulent motion. Domains mainly populated by one of the species emerge, grow, and then split into smaller ones or “melt” back into the mixed phase to make room for growing domains of the concurrent species. To be more specific let us fix an arbitrary point x_0 and record species densities $n_1(x_0, i\tau), n_2(x_0, i\tau), i=1, \bar{N}$, at equal time intervals τ . Constructed in such a way the point trajectory will elucidate the overall dynamics of the system, provided that $N \gg 1$. An example of chaotic trajectory typical of the turbulent medium dynamics in the vicinity of the triple point at $\sigma^2 \approx 4\sigma_c^2$ is presented in Fig. 8. The trajectory was sampled during $3 \cdot 10^5$ elementary time steps and then smoothed over fast small-amplitude oscillations. Note that the trajectory walks freely through the boundaries of the attraction basins spending roughly the same time in the vicinity of each stationary state.

V. OCCUPATION OF AN INITIALLY UNPOPULATED HABITAT

Although all the phenomena mentioned so far are typical of the model (6), they do not cover the whole range of possible dynamical regimes. In the majority of examples it was implied for simplicity that the corresponding coefficients of competitors are to a large extent symmetrical. However, in a natural ecosystem the situation may be different, when each species dominates in some features, but falls behind in the others. Strengths and weaknesses compensate each other, thus, maintaining a stable balance of species. In such a situation one may expect significant complication of the system behavior. The contradiction of the effects of different parameters on the overall fitness of species also enhances the role

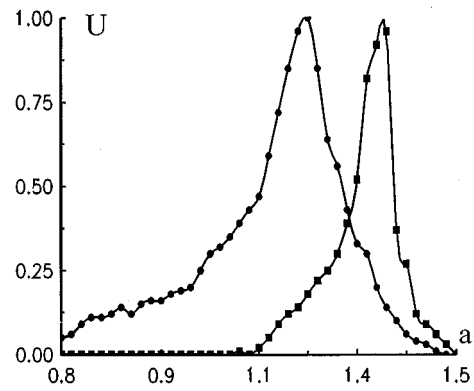


FIG. 9. Uncertainty of the species competition result, $\sigma_{in}^2 = 10^{-6}$. Left curve — $\sigma^2=0$, right curve — $\sigma^2=\sigma_{in}^2$.

of chance. Numerical experiments show that in some special cases it may result in the absolute unpredictability of dynamics.

Let us consider the following scenario. A large, initially unpopulated continuous habitat (e.g. ploughed or burnt out land) is randomly sown by two competing species. One of them, say, the first, breeds faster ($\rho > 0$), but suffers from overcrowding more than the other ($a > b$). It is assumed that initial spatial distributions of species are well approximated by a Gaussian white noise with vanishing intensity $\sigma_{in}^2 \ll 1$. Parameters a, b are chosen from inside the bistable domain, so one of the species is doomed to become extinct. The problem is which species will win? Numerical simulations have revealed the phenomenon of kinetic overshoot, when the faster breeding first species wins although the parameters according to the phase diagram lie deep in the region where the second species is asymptotically stable. Due to this effect the parametric space domain where the first species dominates may enlarge significantly. But what is even more interesting is that the very result of competition becomes a random variable. Different realizations of noisy initial conditions with the same σ_{in}^2 lead to different results. Provided the faster breeding first species outnumbers the second one everywhere in the habitat during the growth process, it wins. But if the second one is able to form at least one finger-like nucleus which breaks through, it will occupy the whole habitat. To characterize the uncertainty of the result of competition the following measure can be proposed. Let p_i be the probability that the i th species wins, then

$$U = \frac{\min(p_1, p_2)}{\max(p_1, p_2)}$$

takes its maximum value 1, if both results are equally probable: $p_1 = p_2 = 1/2$, and its minimum value — 0, if the result is fully predictable. Distributions of U versus the parameter a for the case $b=0.5, \rho=0.1, \sigma_{in}^2 = 10^{-6}$ are given in Fig. 9 with each point being calculated from 100 trials. The left curve corresponds to the completely deterministic model dynamics. Analogous results have been reported earlier¹⁷ for the classical model as well. The right curve presents the data with white noise applied (in the same way as it is described

in Sec. IV). Though $\sigma^2 = \sigma_{in}^2 = 10^{-6}$, the differences are noticeable. It may seem surprising, but noise “helps” the faster breeding species. To account for this effect one should take into consideration the dependence of the individual fertility on the population density at low n_i . Leaving only linear and quadratic terms in Eqs. (6) we obtain:

$$\begin{aligned} \dot{n}_1 &= (1 - \beta_1 + \rho)n_1 + (\beta_1/\alpha_1 - a)n_1^2 - n_1n_2 + D_1\Delta n_1, \\ \dot{n}_2 &= (1 - \beta_2 - \rho)n_2 + (\beta_2/\alpha_2 - b)n_2^2 - n_1n_2 + D_2\Delta n_2. \end{aligned} \quad (12)$$

Thus, for sufficiently low n_i and $\beta_1/\alpha_1 > a, \beta_2/\alpha_2 > b$ quadratic terms in the set (12) are positive. This makes growing species extremely sensitive to positive sign fluctuations, with larger effect for outnumbering species because of the quadratic character of the phenomenon.

These results demonstrate that for some parametric regions there exists a domain of initial conditions with nonzero measure in the space of functions bounded in a segment for which the model behavior becomes unpredictable and sensitive to even tiny fluctuations.

VI. CONCLUDING REMARKS

To highlight contributions of the modification made in Sec. II to the system dynamics, model (4),(6) is worth comparing to the classical one. First of all, it should be noted that the model (1) is structurally unstable. Indeed, at parameters $a = 1 + \rho/1 - \rho$, $b = 1 - \rho/1 + \rho$ linear nullclines of the classical model merge resulting in a continuum of stationary points. Any vector function added to the rhs of (1) and perturbing the linear shape of nullclines, no matter how small the modulo of this perturbation, will inevitably lead to the complete disappearance of such bifurcation. Thus, any arbitrary small perturbation not preserving linearity of nullclines changes qualitative behavior of the model drastically. As the classical model is contained in the model (4),(6) as a limiting case at $\alpha_i, \beta_i \rightarrow 0$, no additional effort is needed for its analysis. Combining the points A, B, C, D in one point C^* in Fig. 1, so that the domains 5, 6, 7 disappear completely, one can get the partitioning of the (a, b) plane for the model (1). Thus, in the frame of the classical model the mixed and any of the pure states are not stable simultaneously under any parameters. The point C^* in the (a, b) plane in which all the domains 1, 2, 3, 4 meet is just the one where the model has merging nullclines. In the spatially distributed analog of the model (1) this point becomes a critical one. Qualitatively it can be seen from Fig. 3 where the points A, B, C, D and T should be combined again into one point. The same result can be obtained formally from Eq. (9) by taking the limit $\alpha_i, \beta_i \rightarrow 0$. The reaction term vanishes proportionally to ε and the system can exist only in a spatially homogeneous state. This prohibits the spontaneous emergence of spatial patterns (even noise-induced) in the frame of classical model.¹⁷ From the above discussion the most interesting phenomena evidently take place where inter- and intraspecific competitions are nearly of the same strength ($a, b \approx 1$). In the classical model this parameter domain is completely masked

by strange phenomena originating from the nullclines linearity. The two models can be compared in the following evolutionary aspect. Let us imagine that species coevolve from stable coexistence through strengthening of competition to the exclusion of one of them. According to the classical model the density of that species decreases steadily up to complete extinction. This process occurs as slowly as parameters evolve. However, in the frame of the modified model extinction catastrophes are possible when the entire ecosystem has no time for relaxation. Such an abrupt extinction has been reported as a starting event for the whole avalanches of extinction-speciation phenomena,¹⁸ which can be considered as manifestations of self-organized criticality.¹⁹

In conclusion we wish to stress the organizing role of noise in the system dynamics, as it not only induces the formation of spatial patterns, but also switches on endless turbulent-like rearrangement of the system. Therefore this turbulent condition can be considered as a new, purely noise-induced, stationary state.

ACKNOWLEDGMENTS

The authors thank the Russian Foundation of Fundamental Research for the financial support under Grant No. 94-01-00959. We acknowledge Professor R. Kapral for his interest in this work and helpful comments. In addition A.G. wishes to express his sincere gratitude to K. Temple for her invaluable contribution to the improvement of the style of the present paper.

APPENDIX: THE NONEXISTENCE OF LIMIT CYCLES IN COMPETITION MODELS

Theorem 1. Consider a set of equations:

$$\dot{x} = f(x, y), \quad \dot{y} = g(x, y); \quad (x, y) \in G; \quad f, g \in C^1(G), \quad (A1)$$

where G is a domain in R^2 . Let

$$f'_y g'_x > 0 \quad (A2)$$

everywhere in G .

Then the set (A1) has no limit cycles in G .

Proof. Assume the set (A1) has a limit cycle $\Omega \subset G$.

Then there should be a point $A \equiv (x^{(A)}, y^{(A)}) \in \Omega$, such that for $\forall (x, y) \in \Omega$ $x \leq x^{(A)}$; and also a point $B \equiv (x^{(B)}, y^{(B)}) \in \Omega$, such that for $\forall (x, y) \in \Omega$ $y \leq y^{(B)}$.

The time t can be considered as a value parametrizing a trajectory in the phase plane (x, y) . Thus in the point A

$$\dot{x}^{(A)} \equiv f^{(A)} = 0, \quad \ddot{x}^{(A)} \leq 0 \quad (A3)$$

and

$$\begin{aligned} \dot{y}^{(A)} &\equiv g^{(A)} < 0 \text{ for clockwise motion along the cycle,} \\ \dot{y}^{(A)} &\equiv g^{(A)} > 0 \text{ for counter-clockwise motion.} \end{aligned} \quad (A4)$$

Similarly in the point B

$$\dot{y}^{(B)} \equiv g^{(B)} = 0, \quad \ddot{y}^{(B)} \leq 0 \quad (A5)$$

and

$$\begin{aligned} \dot{x}^{(B)} &\equiv f^{(B)} > 0 \text{ for clockwise motion,} \\ \dot{x}^{(B)} &\equiv f^{(B)} < 0 \text{ for counter-clockwise motion;} \end{aligned} \quad (\text{A6})$$

$$\ddot{x} = \dot{f} = f'_x \dot{x} + f'_y \dot{y} = f f'_x + g f'_y;$$

$$\ddot{y} = \dot{g} = g'_x \dot{x} + g'_y \dot{y} = f g'_x + g g'_y.$$

From (A3) and (A5) we obtain correspondingly

$$\ddot{x}^{(A)} = g^{(A)} f'_y \leq 0 \quad (\text{A7})$$

and

$$\ddot{y}^{(B)} = f^{(B)} g'_x \leq 0. \quad (\text{A8})$$

For both possible types of motion along the cycle (A4) and (A6) give

$$g^{(A)} f^{(B)} < 0. \quad (\text{A9})$$

Finally, comparing inequalities (A7)–(A9) we obtain

$$f'_y \dot{x}^{(A)} g'_x \dot{y}^{(B)} = \frac{\dot{x}^{(A)} \dot{y}^{(B)}}{g^{(A)} f^{(B)}} \leq 0, \quad (\text{A10})$$

which is a contradiction to the condition (A2). Thus the assumption of the existence of a limit cycle is not true.

¹L.A. Segel and J.L. Jackson, *J. Theor. Biol.* **37**, 545 (1972).

²L.A. Segel and S.A. Levin, in *Topics in Statistical Mechanics and Biophysics*, AIP Conf. Proc. **27** (American Institute of Physics, New York, 1976), p. 123.

³G.F. Gause, *The Struggle for Existence* (William and Wilkins, Baltimore, 1934).

⁴A. Okubo, *Diffusion and Ecological Problems: Mathematical Models* (Springer-Verlag, Berlin, 1980).

⁵N. Shigesada, K. Kawasaki, and E. Teramoto, *J. Theor. Biol.* **79**, 83 (1979).

⁶N. Shigesada and J. Roughgarden, *Theor. Pop. Biol.* **21**, 353 (1982).

⁷M. Mimura and K. Kawasaki, *J. Math. Biol.* **9**, 49 (1980).

⁸N.F. Britton, *J. Theor. Biol.* **136**, 57 (1989).

⁹N.F. Britton, *SIAM J. Appl. Math.* **50**, 1663 (1990).

¹⁰M.C. Cross and P.C. Hohenberg, *Rev. Mod. Phys.* **65**, 851 (1993).

¹¹M.I. Dykman, M.M. Millonas, and V.N. Smelyanskiy, *Phys. Lett. A* **195**, 53 (1994).

¹²W.C. Alle, *Animal Agregation: A Study in General Sociology* (Chicago University Press, Chicago, 1931).

¹³H. Haken, *Synergetics. An Introduction* (Springer-Verlag, Berlin, 1978).

¹⁴F. Schlögl, *Z. Phys.* **253**, 147 (1972).

¹⁵A.B. Goryachev, A.A. Polezhaev, and D.S. Chernavskii, *Biofizika* **39**, 726 (1994).

¹⁶W. Horsthemke and R. Lefever, *Noise-Induced Transitions* (Springer-Verlag, Berlin, 1984).

¹⁷A.B. Goryachev, A.A. Polezhaev, and D.S. Chernavskii, *Mat. Model.* (in press).

¹⁸S.A. Kaufmann and S. Johnson, *J. Theor. Biol.* **149**, 467 (1991).

¹⁹P. Bak, C. Tang, and K. Wiesenfeld, *Phys. Rev. A* **38**, 364 (1988).